

Magnetoresistance Oscillations in a Two-Dimensional Electron Gas Induced by a Submicrometer Periodic Potential.

D. WEISS(*), K. v. KLITZING(*), K. PLOOG(*) and G. WEIMANN(**)

(*) *Max-Planck-Institut für Festkörperforschung, Heisenbergstraße 1
D-7000 Stuttgart 80, F.R.G.*

(**) *Walter-Schottky-Institut, TUM, D-8046 Garching, F.R.G.*

(received 29 October 1988; accepted 7 November 1988)

PACS. 72.20M – Galvanomagnetic and other magnetotransport effects.

PACS. 73.60 – Electronic properties of thin films.

PACS. 73.60F – Semiconductor films.

Abstract. – A new type of magnetoresistance oscillation periodic in $1/B$ is observed when the carrier density N_s of a two-dimensional electron gas is weakly modulated with a period smaller than the mean free path of the electrons. Experiments with high mobility AlGaAs-GaAs heterojunctions where N_s is modulated by holographic illumination at $T \leq 4.2$ K show that the period of the additional quantum oscillation is determined by the separation a of the interference fringes. This period corresponds to Shubnikov-de Haas oscillations where only the electrons within the first reduced Brillouin zone with $|k| < \pi/a$ contribute.

At low temperatures the magnetoresistance of a degenerate two-dimensional electron gas (2-DEG) exhibits the well-known Shubnikov-de Haas (SdH) oscillations periodic in $1/B$. Lateral confinement of the 2-DEG on a submicrometer scale leads to deviations from the typical $1/B$ periodicity of these SdH-oscillations [1]. Within a naive picture these deviations occur when the cyclotron orbit of an electron is larger than the width of the confining potential [2]. An intermediate situation between a purely two-dimensional system and a quasi-one-dimensional quantum wire is if the confining potential of the quantum wire is replaced by a periodic potential with a length scale smaller than the mean free path of the electrons. The experiments show that under this condition a new type of magnetoresistance oscillation becomes visible with a periodicity depending on the period of the superimposed potential.

In selectively doped AlGaAs-GaAs heterostructures a persistent increase in the two-dimensional electron density is observed at temperatures below $T = 150$ K if the device is illuminated with infrared or visible light. This phenomenon is usually explained on the basis of the properties of DX-centres which seem to be related to a deep Si donor [3]. The increase in the electron density depends on the photon flux absorbed in the semiconductor so that a spatially modulated photon flux generates a modulation in the carrier density. In our measurements a holographic illumination of the heterostructure at liquid helium tempera-

tures is used to produce a periodic potential with a period in the order of the wavelength of the interfering beams. The existence of a periodically modulated carrier density in such structures has been proved by Tsubaki, Sakaki, Yoshino, and Sekiguchi [4] who measured the anisotropy of the resistivity parallel and perpendicular to the interference fringes. Tsubaki and coworkers stated that the smallest possible period for finding an anisotropic resistivity is four or five times as large as the thickness of the AlGaAs layers. Since we have created smaller fringe periods we have observed nearly isotropic resistivity at zero magnetic field. In the presence of a magnetic field, however, a new oscillatory phenomenon occurs demonstrating clearly that a periodic modulation of the 2-DEG is present.

The samples used in this work were conventional AlGaAs-GaAs heterostructures grown by molecular beam epitaxy [5] with carrier densities between $1.5 \cdot 10^{11} \text{ cm}^{-2}$ and $4.3 \cdot 10^{11} \text{ cm}^{-2}$ and low-temperature mobilities ranging from $0.23 \cdot 10^6 \text{ cm}^2/\text{Vs}$ to $1 \cdot 10^6 \text{ cm}^2/\text{Vs}$. Illumination of the samples increases both the carrier density and the mobility at low temperatures. The heterojunctions discussed in this letter consist of a semi-insulating GaAs substrate, followed by a $(1 \div 4) \mu\text{m}$ thick undoped GaAs layer, an undoped AlGaAs spacer $((6 \div 33) \text{ nm})$, Si-doped AlGaAs $((33 \div 84) \text{ nm})$, and an undoped GaAs top layer $(\approx 22 \text{ nm})$. For an analysis of the magnetotransport properties parallel and perpendicular to the interference fringes an L-shaped sample geometry was chosen (sketched on the right-hand side of fig. 1). Such a mesa structure was produced using standard photolithographic-and

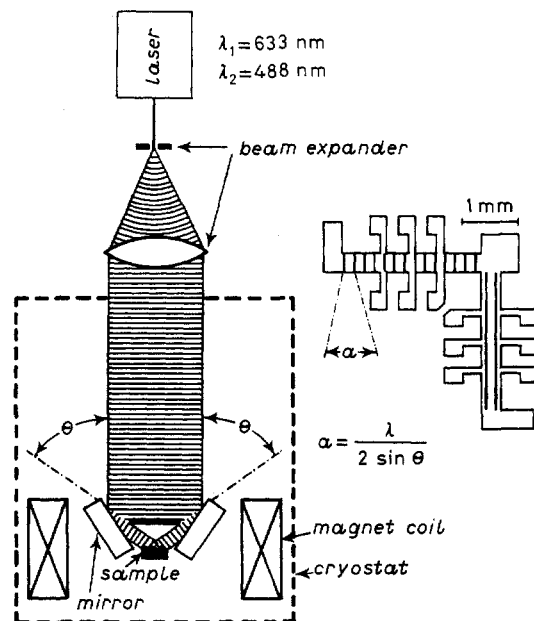


Fig. 1. – Schematic experimental set-up (left-hand side) and top view of the L-shaped sample geometry where the interference pattern is shown schematically.

etch techniques. Ohmic contacts to the 2-DEG were formed by alloying AuGe at 450°C . Some of the samples investigated have an evaporated semi-transparent NiCr front gate (thickness $\approx 8 \text{ nm}$) to vary the carrier density after holographic illumination. The experiment was carried out using either a 5 mW HeNe laser ($\lambda = 633 \text{ nm}$) or a 3 mW argon-

ion laser ($\lambda = 488$ nm) both linearly polarized. The schematic experimental set-up is shown in fig. 1. The laser system was mounted on top of the sample holder which was immersed in liquid helium (4.2 K) within a 10 T magnet system. The laser beam which was expanded to a diameter of 40 mm entered the sample holder through a quartz window and a shutter. The shutter ensures well-defined illumination times of the sample down to 25 ms. Short exposure times are important to prevent jumping of the fringes; therefore exposure times between 25 ms and 100 ms were typically chosen. The mirrors which split the laser beam into two coherent waves are located close to the device and are arranged in such a way that an interference pattern with a period a is generated at the surface of the device. The period a depends on the wavelength λ of the laser and the incident angle θ (see fig. 1): $a = \lambda/2 \sin \theta$. With the wavelengths used in this experiment and $\theta = 56^\circ$ we obtain periods of 382 nm and 294 nm. All inner parts of the sample holder were coated with an absorbing layer in order to minimize stray light from the laser beam. The optical components of the experimental set-up have a wavefront distortion better than $\lambda/10$, where λ is the wavelength of a HeNe-laser ($\lambda = 633$ nm).

After holographic illumination of the sample the resistivities ρ_{\perp} (perpendicular to the interference fringes) and ρ_{\parallel} (parallel to the fringes) were measured at low temperatures as a function of the magnetic field perpendicular to the plane of the 2-DEG. The resistivity is measured applying a constant current ($1 \div 10$) μA and measuring the voltage drop between potential probes along the direction of current flow. A typical result is shown in fig. 2. At

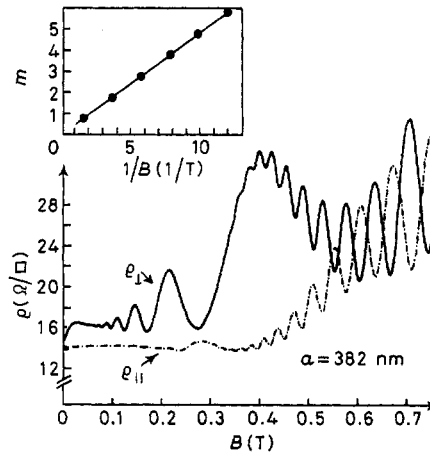


Fig. 2. - Magnetoresistivity ρ parallel and perpendicular to the interference fringes. $T = 2.2$ K, $N_s = 3.16 \cdot 10^{11} \text{ cm}^{-2}$, $\mu = 1.30 \cdot 10^6 \text{ cm}^2/\text{Vs}$. The inset displays the $1/B$ behaviour of the additional oscillations where the points correspond to minima of ρ_{\perp} , slope: $n = 2.35 \cdot 10^{10} \text{ cm}^{-2}$.

magnetic fields higher than 0.3 T both ρ_{\perp} and ρ_{\parallel} show well-known SdH-oscillations with a periodicity $\Delta(1/B)$ inversely proportional to the 2-DEG carrier density N_s . Below 0.3 T pronounced additional oscillations dominate ρ_{\perp} , while weaker oscillations with a phase shift of 180° relative to the ρ_{\perp} -data are visible in the ρ_{\parallel} measurements. The oscillations in ρ_{\perp} are accompanied by a remarkably positive magnetoresistance at very low magnetic fields. The additional oscillatory structures are much less temperature sensitive than the SdH-oscillations, ruling out the possibility that these oscillations are due to an occupation of the first subband. Increased exposure times smear out the interference fringes; continuous

illumination, therefore, always destroys the additional oscillations at low magnetic fields. Since the additional oscillations in ρ_{\perp} are perfectly periodic in $1/B$ (see inset of fig. 2) the periodicity can be expressed as a carrier density n . Analogous to SdH-oscillations one obtains (spin splitting not resolved)

$$n = \frac{e}{\pi \hbar} \left(\Delta \frac{1}{B} \right)^{-1}. \quad (1)$$

Here e is the elementary charge, \hbar is Planck's constant and $\Delta(1/B)$ is the difference between adjacent minima (or maxima) of ρ_{\perp} or ρ_{\parallel} on a $1/B$ scale. From the SdH-oscillations (also using eq. (1)) as well as from low-field Hall measurements an average carrier density N_s can be obtained. The carrier density N_s and mobility μ measured parallel and perpendicular to the interference pattern are equal within 5%. Since, in addition, we do not observe additional structure in the higher-field regime of ρ_{\perp} and ρ_{\parallel} due to a second carrier density, we conclude that we have only a weak modulation of the carrier density. This means that the amplitude of the additional periodic potential introduced by holographic illumination is small compared to the Fermi energy of the system. Using a semi-transparent top gate or a back gate the carrier density N_s can be varied further after producing the interference fringes. Changing the carrier density N_s results in a change of the periodicity of the additional oscillations in ρ_{\perp} and ρ_{\parallel} ; as N_s increases, $\Delta(1/B)$ decreases and therefore n increases, too. The period of the additional oscillations, however, depends not only on N_s but also on the period of the holographically defined periodic potential; using a smaller period a results in a higher n at fixed carrier density N_s . These results obtained for a fringe period of 294 nm and 382 nm are

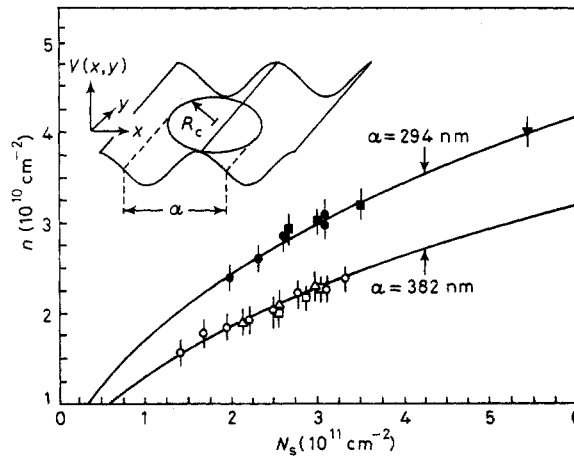


Fig. 3. - n vs. carrier density N_s . Full symbols correspond to a wavelength $\lambda = 488$ nm, open symbols to $\lambda = 633$ nm and different symbols represent different samples. The solid lines are calculated using the condition that the cyclotron orbit diameter $2R_c$ is equal to an integer multiple of the interference period a , as sketched in the inset.

summarized in fig. 3, where n is plotted as a function of the carrier density N_s . The lines in fig. 3 are calculated curves without any free parameter based on the assumption that the period is simply given by the condition that the classical cyclotron orbit is equal to an integer

number of fringe periods a (visualized in the inset of fig. 3):

$$R_c = \frac{m^* v_F}{e B} = \frac{a}{2}(m + \varphi), \quad m = 1, 2, 3, \dots \quad (2)$$

R_c is the cyclotron radius, v_F is the electron velocity at the Fermi energy, m^* is the electron effective mass and φ is a phase factor. Substituting for v_F using $v_F = \hbar k_F / m^*$, we can rearrange eq. (2) to obtain

$$\Delta \frac{1}{B} = e \frac{a}{2\hbar k_F} \quad (3)$$

and calculate n using eq. (1) and the relation $k_F = (2\pi N_s)^{1/2}$. This simple picture is in excellent agreement with the experimental data. The picture described above demands an elastic free path l_e at least as long as the perimeter of the cyclotron orbit. This agrees with our finding that the number of oscillation periods depends on the mobility of the sample; the higher the mobility, the more oscillations are observable. From the mobility of the sample used in the measurements of fig. 2 a mean free path of 12 μm can be calculated in agreement with the estimated cyclotron orbit perimeter of 11 μm for the largest cyclotron orbit which produces a structure in the ρ_{\perp} curve at about 0.054 T ($m = 9$ in fig. 2).

If maxima in the ρ_{\perp} curves are interpreted as maxima in the scattering rate than the experimentally determined phase shift $\varphi = 0.17 \pm 0.06$ in eq. (2) means that the strongest interaction of the cyclotron motion with the periodic potential occurs if the diameter of the cyclotron orbit is 0.17 a larger than an integer multiple of the period a . On the other hand, minima occur when $\varphi = -0.25 \pm 0.06$. It should be mentioned that this effect seems to be similar to the magnetoacoustic resonance [6, 7]; the detailed mechanism, however, which results in minima in ρ_{\perp} , while at the same magnetic field ρ_{\parallel} displays maxima remains unclear at the moment.

The period of the additional oscillations can be described in a more quantum-mechanical picture. The additional periodic potential introduces new Brillouin zones where in one direction $-\pi/a$ and π/a form the boundary of the first Brillouin zone, while in the other direction the electron states are occupied up to k_F . We observe that the carrier density which fills the first reduced Brillouin zone is equal to that connected with the additional oscillations.

In summary we have reported a new type of magnetoresistance oscillation, the periodicity of which can be equally well described either by the condition that the classical cyclotron orbit equals an integer multiple of the periodic potential period or in terms of the carrier density required to fill the first reduced Brillouin zone of the modulated system.

* * *

We would like to thank D. HEITMANN and R. R. GERHARDTS for stimulating suggestions and discussions and S. BENDING and A. MACDONALD for critically reading the manuscript.

REFERENCES

- [1] BERGGREN K.-F., THORNTON T. J., NEWSON D. J. and PEPPER M., *Phys. Rev. Lett.*, **57** (1986) 1769.
- [2] VAN HOUTEN H., VAN WEES B. J., MOOIJ E. J., ROOS G. and BERGGREN K.-F., *Superlattices and Microstructures*, **3** (1987) 497.
- [3] SCHUBERT E. F., KNECHT J. and PLOOG K., *J. Phys. C*, **18** (1985) L-215.
- [4] TSUBAKI K., SAKAKI H., YOSHINO J. and SEKIGUCHI Y., *Appl. Phys. Lett.*, **45** (1984) 663.
- [5] SCHUBERT E. F. and PLOOG K., *Appl. Phys. A*, **33** (1984) 63.
- [6] PIPPARD A. B., *Philos. Mag.*, **2** (1957) 1147.
- [7] COHEN M. H., HARRISON M. J. and HARRISON W. A., *Phys. Rev.*, **117** (1960) 937.